UNIVERSITY OF TARTU
Faculty of Science and Technology
Institute of Technology

Rufat Abdullayev

The Comparison of three Reconstruction methods: Straight line, Point of the closest approach (POCA), Maximum likelihood expectation maximization (MLEM)

Bachelor's Thesis (12 ECTS)

Supervisor(s): Leonid Zinatullin

Tartu 2025

Resumee/Abstract:

Kolme rekonstrueerimismeetodi võrdlus (sirgjoon, lähima lähenemise punkt (POCA), maksimaalse tõenäosuse ootuse maksimeerimine (MLEM))

Muontomograafia pakub tõhusat võimalust suurte ja raskete objektide sisemuse kujutamiseks, kasutades kosmilisi kiirgusmuone. Antud töö on võrdlev uuring, mis esitleb kolme rekonstrueerimisinstrumendi: lähima lähenemise punkti (POCA), sirgjoone ja maksimaalse tõenäosuse ootuse maksimeerimise (MLEM) kasutatavust muontomograafias. Nende instrumentide tõhusust ja täpsust hinnatakse GEANT4 tööriistakomplekti simuleeritud andmete põhjal. Simulatsiooni seadistus on lähedane reaalsetele eksperimentaalsetele tingimustele: kuus virtuaalset andurit on paigutatud objekti kohale ja alla, et jälgida muonide trajektoore. POCA tehnika määrab hajumiskeskused, arvutades lähima lähenemise punktid sissetulevatele ja väljuvatele muonidele. Sirgjoone tehnika eeldab, et muonide rajad on lineaarsed. See valib punkti viimase sissetuleva ja esimese väljuva punkti keskel. MLEM tehnika on iteratiivne ja täiustab iteratiivselt kujutist, maksimeerides vaadeldud andmete tõenäosust. Kuigi POCA meetod ja sirgjoon on efektiivsed arvutusmeetodid, on MLEM täpsem kui need, eriti kui vaadata heterogeensetes keskkondades rakendamist. See näitab iga meetodi plusse ja miinuseid ning aitab tuvastada ideaalseid muontomograafia protsesse, mis hõlmavad arheoloogilisi uurimisi, tuumajulgeolekut ja tööstuslikku kontrolli.

Võtmesõnad:
sirgjoon, GEANT4, POCA, MLEM

CERCS:
P160: Statistika, operatsioonanalüüs, programmeerimine, finants- ja kindlustusmatemaatika;
T111: Pilditehnika

The Comparison of three Reconstruction methods (Straight line, Point of the closest approach (POCA), Maximum likelihood expectation maximization (MLEM)) Muon tomography offers an effective opportunity to image the inner parts of big and heavy objects by using cosmic ray muons. This is a comparative study that presents the performance of the three reconstruction instruments: Point of Closest Approach (POCA), Straight Line, and Maximum Likelihood Expectation-Maximization (MLEM) in muon tomography. The efficacy and accuracy of these instruments are assessed by simulating data that is the resulting effect of the GEANT4 toolkit. The setup of the simulation is close to the real experimental conditions: six virtual sensors are set above and beneath the object to pick the trajectory of the muons. The POCA technique gives the assignment of the scattering centers by computing the points of closest approach for the incoming and outgoing muons. The Straight Line technique assumes that the muon paths are

linear. It selects the point in the middle of the last incoming and the first outgoing points. The MLEM technique is iterative and refines an image iteratively by maximizing the likelihood of the observed data. While the POCA method and the Straight Line are methods for efficient computation, the MLEM is more accurate than they are, in particular when regarding the application in media that are this heterogeneous. It will display the pros and cons of each method and help in identifying the ideal muon tomography processes, which will cover archaeological investigations, nuclear security, and industrial inspection.

Keywords:
POCA, MLEM, Straight line, GEANT4

CERCS:
P160 Statistics, Operation Research, Programming, Actuarial Mathematics;
T111 Imaging, Image Processing

Contents

1 Abbreviations

VOI – Volume of Interest

POCA – Point of Closest Approach

MLEM – Maximum Likelihood Expectation Maximization

GEANT4 – Geometry and Tracking version 4 (a toolkit for the simulation of the passage of particles through matter)

Z – Atomic Number (used to denote density or type of material in this context)

3D – Three-Dimensional

2D – Two-Dimensional

cm – Centimeter

mm – Millimeter

Fe – Iron (Element Symbol)

2 Introduction

Getting information about the internal structure of an object without harming it is an important aspect for many scientific and industrial applications. For this reason, X-rays are commonly used in many areas due to being easy to use, but it has limitations, such as limited penetration through dense materials, potential damage risks to the object, and inability to cover large distances. For that reason, in some areas, the usage of muons - high-energy cosmic particles that continuously pass through the Earth's atmosphere - has become popular.

Cosmic-ray muons are, in fact, existing particles that, for that matter, can be said to be similar to electrons, but are, on the other hand, much more massive. They can sometimes just traverse meters of either rock or metal, which loses their kinetic energy gradually because they are in the process of colliding with atoms of that material. By this property, they can pass through heavy objects that would appear opaque to different kinds of radiation, like X-rays or gamma rays. The feature that allows them to lose kicks of energy in this way creates a level of detail in the structure of an object that can be turned into an image by measuring and analyzing them as they exit from the object being passed through.

Muon tomography is an imaging modality to inspect the internal structure of bulky and dense objects with the help of cosmic-ray muons. Since these subatomic particles are produced by continuous interaction between cosmic rays and the Earth's atmosphere, they have the peculiarity of percolating through a thick material. Such capacities of penetration make muon tomography adaptable to a number of good applications in the sphere of non-invasive imaging in the widest range of sciences and industries. One of the early applications of this concept was done by Luis Alvarez and his team in 1970[1], in which the team was trying to detect hidden chambers in the Second Pyramid of Giza and learn more about the structure of the Second Pyramid of Giza. Even though hidden chambers could not be detected with this research due to the limitations of computational power back in time, the potential applications of Muon tomography for archaeological exploration were clearly shown in this research. During the following decades, Muon tomography played a great role in studying Archaeology[2] and Geoscience applications[3, 4].
With the development of detector technology and computing power, the capability of muon tomography has significantly enhanced. As a result of that, the technology has been employed in some notable projects in the previous years with success. For example, researchers employed the method of muon radiography in 2010 to study the internal structure of Mount Etna (Italy), enabling low-risk, high-resolution imaging that could determine the prospective volcanic risks in the region [5]. Tanaka followed a similar study in 2010, where two detectors were employed around Mount Asama to generate

3D images and identify low-density regions around the crater [6]. Muon tomography has also been employed outside the volcanology field in some applications, such as the structural analysis of pyramids [7], underground railroads [8], and other hard-to-image infrastructures [9].

Further, muon tomography has proven to be a valuable tool in the fields of nuclear security and energy applications. It has been employed heavily to identify and characterize nuclear threats [10, 11], track spent fuel and nuclear waste [12, 13], and produce 3D representations of nuclear reactors [14]. Overall, the application of muon tomography ranges from archaeology to building stability assessment [15, 16], demonstrating its versatility and growing importance as technological advancements further enhance its precision and performance.

The efficiency of muon tomography primarily depends on the algorithms used for object inner structure reconstruction from collected data about muons. Different algorithms were developed, with their advantages and weaknesses. In this work, the three most well-known reconstruction techniques are considered: Point Of Closest Approach (POCA), Straight Line, and Maximum Likelihood Expectation Maximization (MLEM). The Point Of Closest Approach (POCA) seeks the places where the trajectory of the incident and exiting muons is closer to one another. This algorithm is cheap in computing resources and relatively easy to implement. Its accuracy might be degraded in complex scenarios, which[17] include multi-scatterings[15].

Under idealized conditions, the Straight Line algorithm assumes that the muons travel in the object along straight lines. It reconstructs the inner object structure with the use of the middle point between the last point of entrance and the first point of exit of the muon trajectory. This approach is simple and computationally fast. At the same time, it doesn't produce suitable results in the cases of significant scattering.

The Maximum Likelihood Expectation Maximization (MLEM) algorithm is essentially a solution to an iterative problem to correct the existing image. Since maximization of the likelihood that the real data is maximally suitable to the acquired model, such an approach can handle the inhomogeneities better and reach higher accuracy. It requires very high power, though.

2.1 Muon tomography working principle

This section provides information about the working principle of muon tomography.

One of the most popular and common material for detecting Muons passing through are Scintillators due to the reason that they are very good for muon detection because they emit light proportional to the energy deposited, which is a good match to the muon charge. Organic scintillators — typically plastic — are fast, low-cost, and do not require

complex manufacturing processes, all of which are important advantages in building large-area muon detectors. Their response times in the nanosecond range and adequate attenuation lengths lead to efficient timing for signal collection. Such properties make scintillators a solid, scalable candidate for muon detection.[18]

An example of the layout of a Muon detector can be seen in Fig.1(a), where each detector contains orthogonal double-layer scintillator trackers in a Geant4 simulation to acquire information about muon momentum and energy deposited by Muons [19].

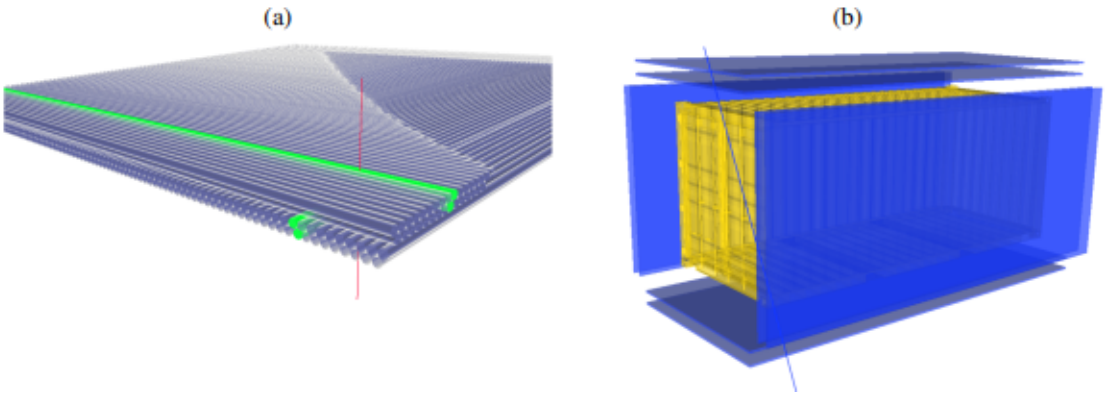

Figure 1. The example of architecture of detector [19]

One example of muon tomography working principle is demonstrated in Fig.2 . Each muon passes through upper and lower detectors, and the xyz coordinates of the Muon when it passes these detectors are recorded as data. Then the data gathered from upper and lower detectors are used as 2 vectors(Incoming and Outgoing), which are later used for trajectory estimation within the container. We are gathering Eventid, which corresponds to each muon individually, (xyz) coordinates of the Muon, and time of the Muon passing through detectors, but we are using only Eventid and (xyz) coordinates to estimate the trajectory of the Muon within a container. Also, because it is a simulation, we have the data of how the muon passed, which we will use to compare with our estimation, giving us an estimation of the error rate in our trajectory estimation.

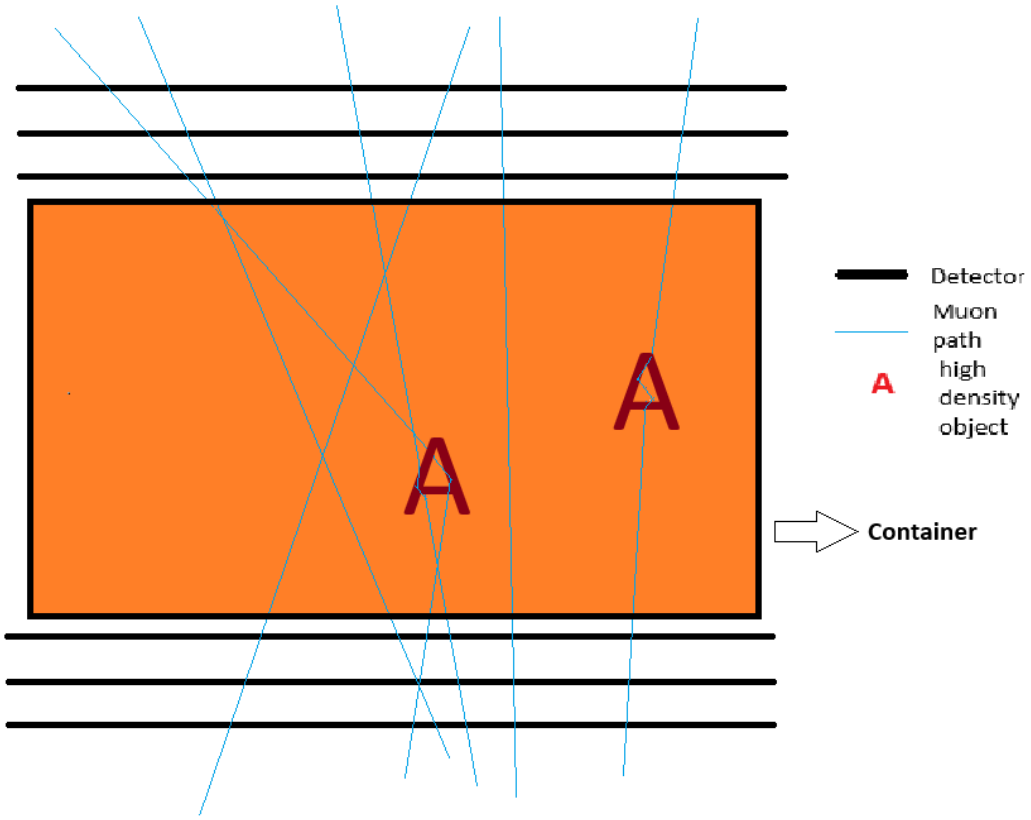

Figure 2. The muon tomography example

2.2 Objectives and Roadmap

In this thesis, it will be tested whether the three mentioned reconstruction methods will be effective and reliable to use on simulated muon tomography data, which is achieved with the help of the GEANT4 toolkit. GEANT4 is a full software to simulate the process of particles' interaction with matter. It has become ubiquitous software in high-energy physics, medical physics, and space science. The simulations carried out for the present work are approximately realistic. In them, there are six virtual sensors above and below the object that register muon trajectories. The distance between the sensors is 10 cm to capture enough detail from the muon's path through the object.

3 The Reconstruction Methods and Algorithm

This section presents the explanation of these 3 reconstruction methods and the algorithm to apply them to our Data.

3.1 Straight line..

The straight line method is the simplest and easiest method among these three methods, as there is almost no computational process for implementing this method, which makes it suitable for rapid imaging. But the accuracy is really low as it just takes the muon path as a straight line, which is completely opposite of how muons move and pass through objects[20].

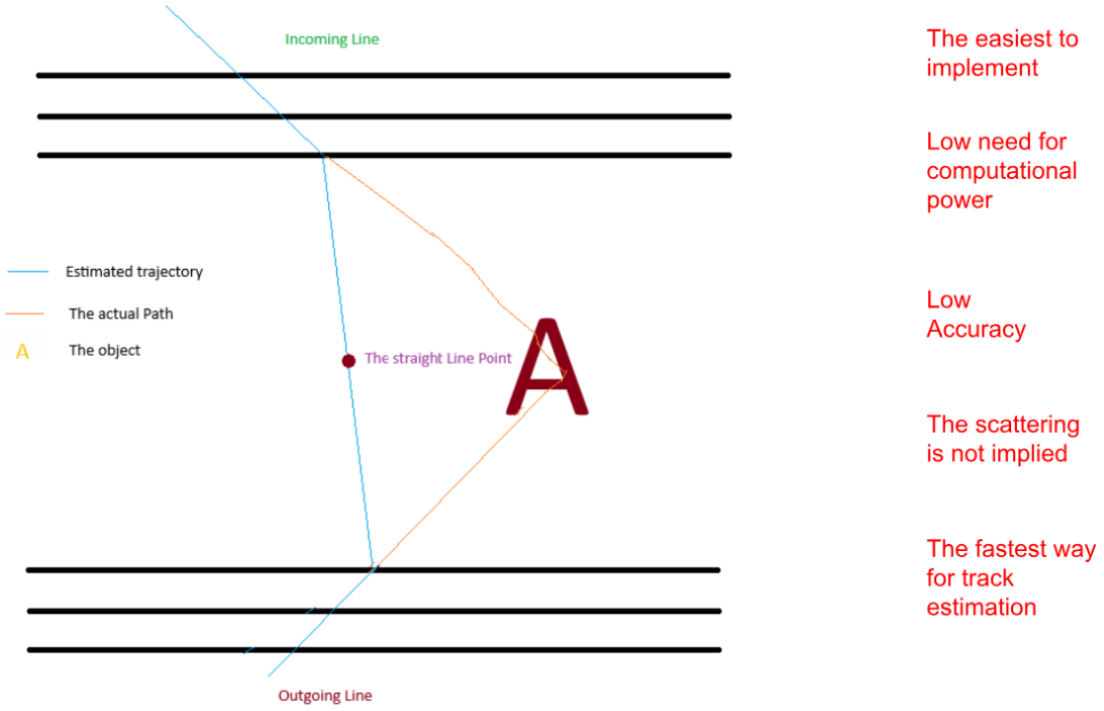

Figure 3. Straight line method.

As we can see in Fig.3, the Straight line method can give completely different results, especially in cases where scattering happens a lot.

3.2 POCA

Point of Closest Approach (POCA) is one of the most basic methods for estimating the muon trajectory in muon tomography. It traces the incoming and outgoing dosed muon (as recognized by the detectors) and computes the position where these two paths come closest to intersection or overlap. POCA assumes the point of closest approach is where the most significant scattering event happens, and uses it to infer the internal structure of the object. Where POCA shines is in simple implementations that require low computational programming. Of course, simplicity comes at a cost, with low accuracy and high chances of false positives, especially in the case of low-Z materials where the basic scattering mechanisms are weak and more difficult to identify [21].

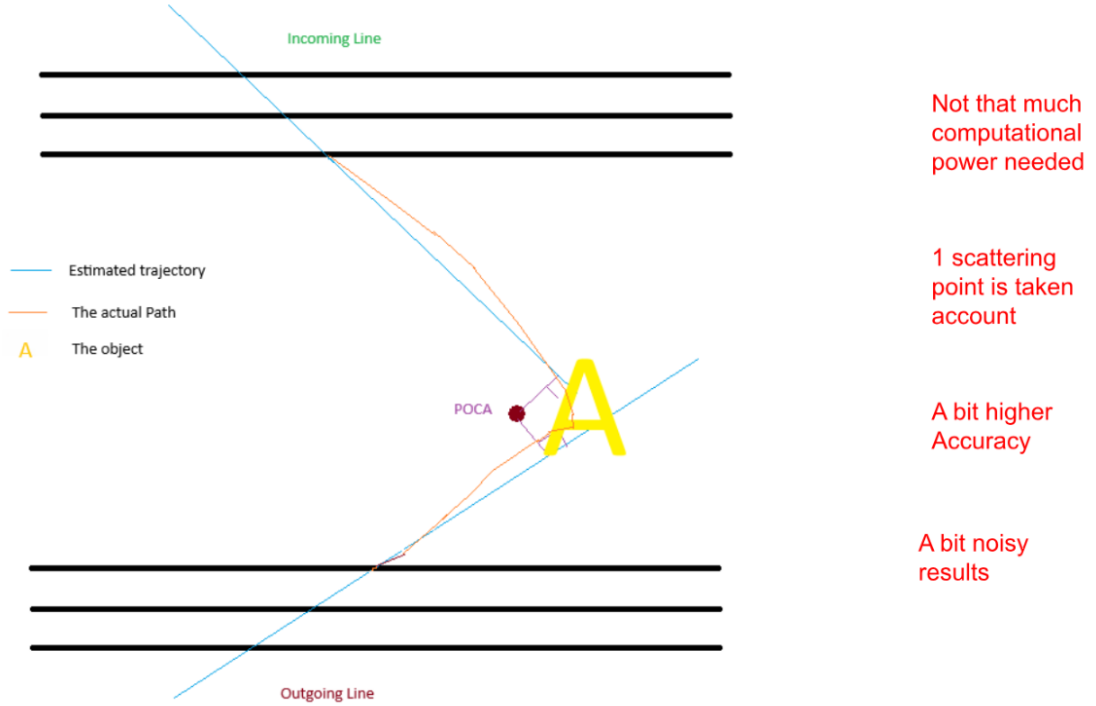

Figure 4. Point of the closest approach(POCA).

Fig.4 demonstrates the example of POCA track path estimation. While this estimation is usually more accurate than the Straight line estimation, it still contains a drawback of taking only account of single scattering.

3.3 MLEM

In different cases where the accuracy needs to be high, the researchers use Maximum-Likelihood Expectation Maximization to reconstruct images[22]. MLEM is a statistical iterative method that attempts to infer the scattering density distribution throughout the scanned volume by maximizing the likelihood that the observed muon-scattering data would be produced by that distribution. Beginning from a guess as to the image, MLEM adjusts the values of the voxels so that the predicted scattering along paths of muons matches the observed scattering angles; the process incrementally and iteratively improves its approximation to an image that best accounts for the data. But still, this method has drawbacks such as being computationally intensive, complex to implement. Therefore, it is not suitable for rapid imaging[21].

3.4 The structure of data processing workflow

Algorithm 1

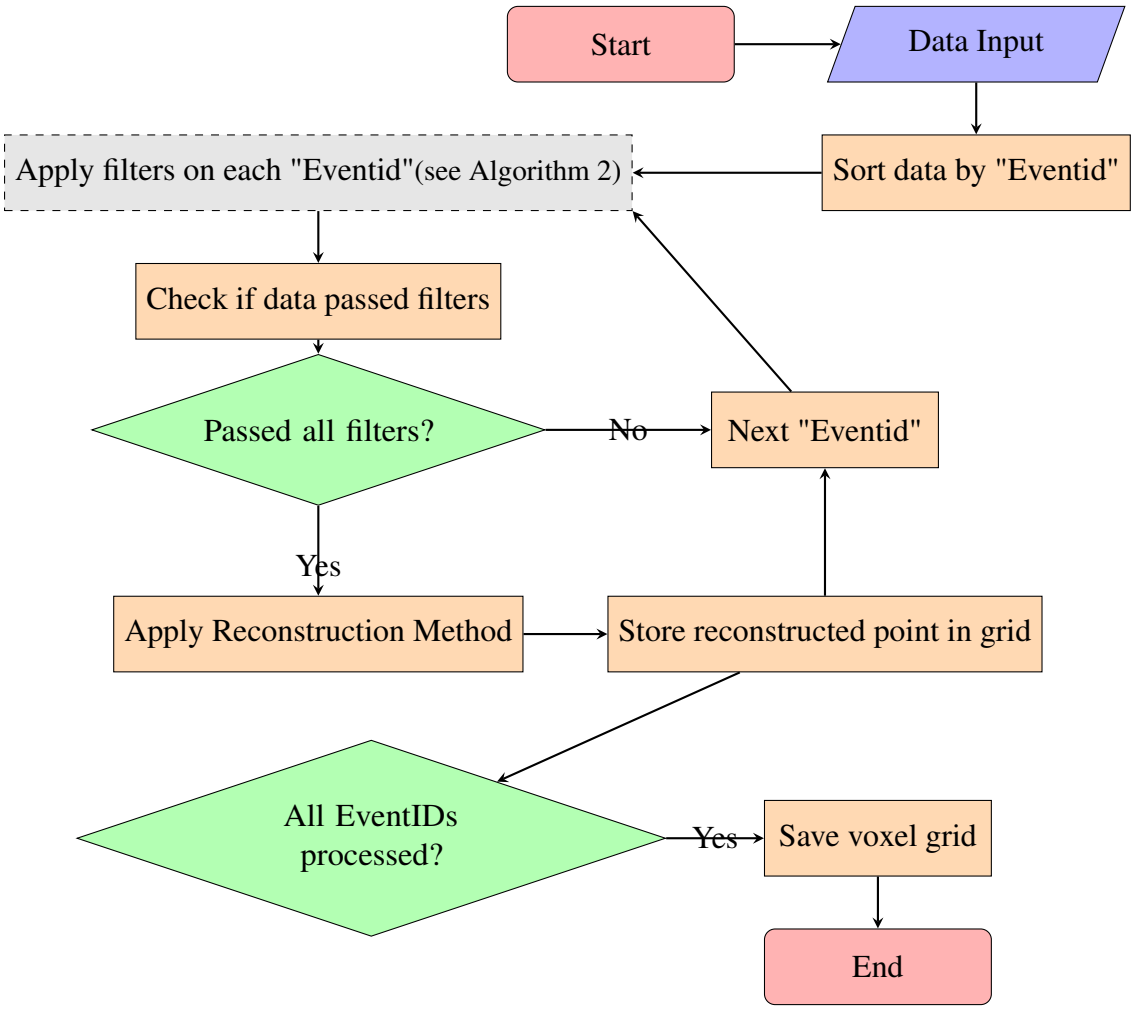

The complete path for processing muon tracking data is given in Algorithm 1. Once data has been uploaded, we group events by "EventID," and then execute a filter step (as explained in Algorithm 2). Once an event survives all filters, the muon scattering point is reconstructed using a fitting method (i.e., POCA or straight-line model). This point is then accumulated on a voxel grid. This is repeated for each event, and when all events are processed, this final voxelised grid is saved and analysed.

Algorithm 2

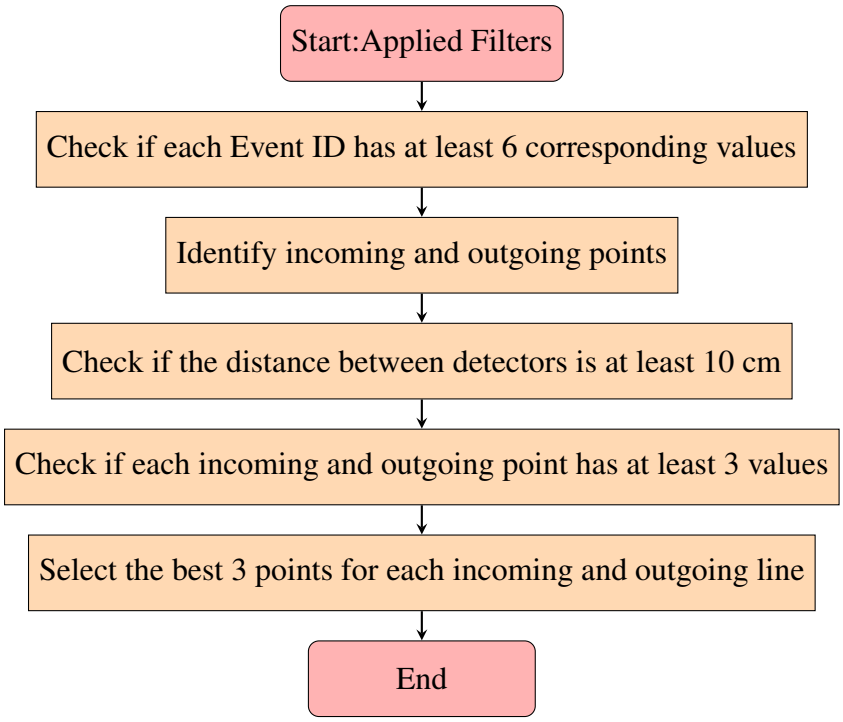

The quality cuts used in the reconstruction are summarised in Algorithm 2. These are checks that the event has more than six hits, a minimum separation of 10 cm between hits in different detector layers, and that there are at least three points for incoming and outgoing tracks. The three best points are then chosen to satisfy the trajectory of the muon. These cuts help to reduce the contamination by noisy spatio-temporal sub-structures when reconstructing the events.

4 Results and Discussion

The results of the 3 reconstruction methods are shown and discussed in this section. The reconstruction methods are tested on synthetic data, which is generated using the simulation in Geant4. More information about the simulation setup and objects is written in Methodology 5.3.

4.1 Straight Line

4.1.1 3d ground truth simulation vs Straight line simulation

While going through the phase of restriction, the ground truth points are used; they are termed as the transport points, which are physically applied while enforcing and testing the fidelity of the reconstruction algorithms. The transport points show the actual paths of the Muons within the container, enhancing the availability of more information in reconstruction. By this, we can calculate the error rate between the paths that are made of transport points and the implemented reconstruction method point. In Fig.5, the visual comparison between the actual path (a) and the Straight line path(b) of one muon is demonstrated.

[a]

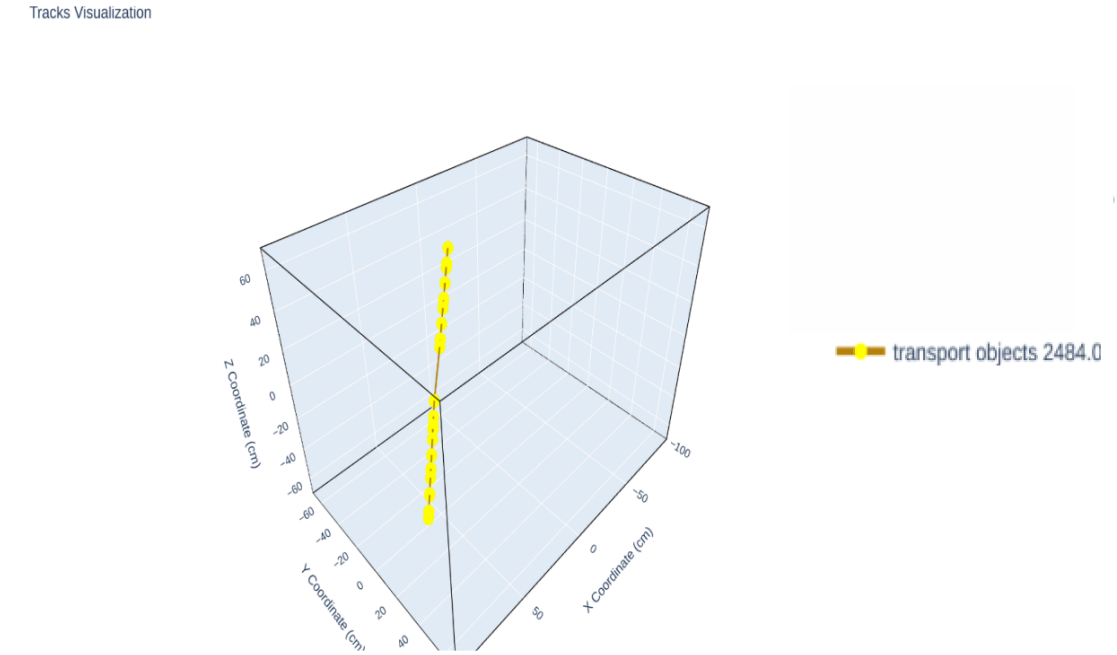

[b]

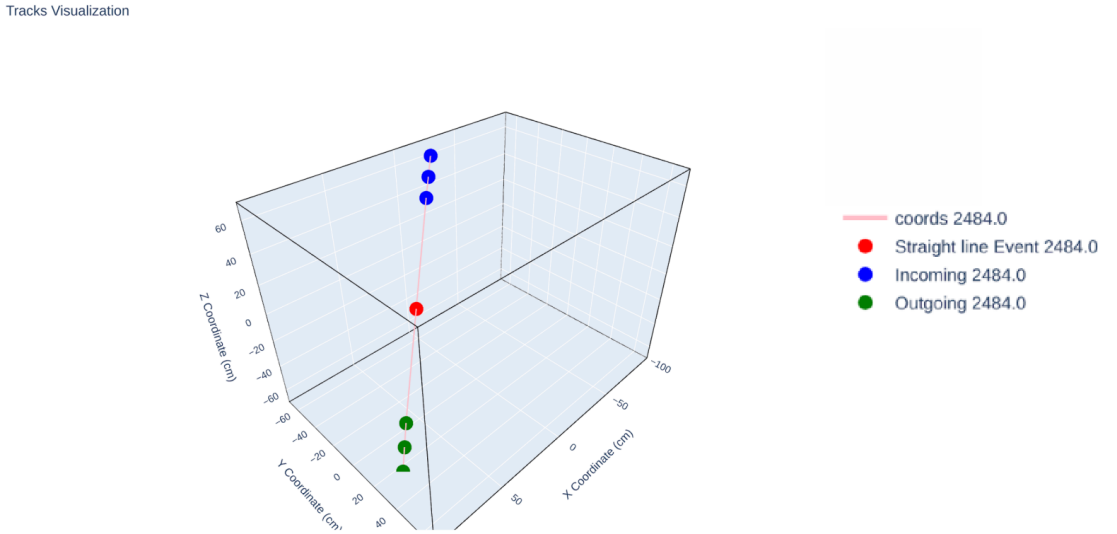

Figure 5. The visual comparison between the actual path and the straight line path. (a) the actual path; (b) the straight line path

The Actual path and Straight line Path are visually too similar in Fig.5. As well as these, the visual comparisons for other Muon examples also show similar results, and the Actual path for most of the muons almost has no scattering angles, which can be an

indicator of errors in the data that is acquired using the Geant4 Monte Carlo simulation package.

4.1.2 The error rate between the actual path and the straight line path

The differences between the fitted lines on The Straight line muon paths and the actual muon paths are measured. The comparison of the fitted lines and transport points gives a test of the Straight line method's accuracy in the reconstruction. In the table.1 The average error rate in centimeters between the actual path and the Straight line path is demonstrated.

Event_id	Average error
5	0.0028945
9	0.3717289
38	0.03074
79	0.005137
125	0.015007
741	0.030473
1148	0.051194
1943	0.118003
2208	0.021995
2484	1.106311

Table 1. The average error rate between actual and straight line paths in centimeters(cm)

The results are in the table.1 shows how the actual and straight line paths are so similar, as the error rates are too low. This outcome also corresponds to the 3D visual comparison in Fig.5.

4.1.3 The density map with voxel slices

After a considerable part of the data is processed and Straight line points acquired, the Straight line points that are collected are added to the voxel grid. The voxel slices work as a 2D density map, which gives visualization and information about the objects inside the simulation. In Fig.6, the voxel slice examples in XY, YZ, and ZX are demonstrated for visualizing the reconstruction with the Straight line Method.

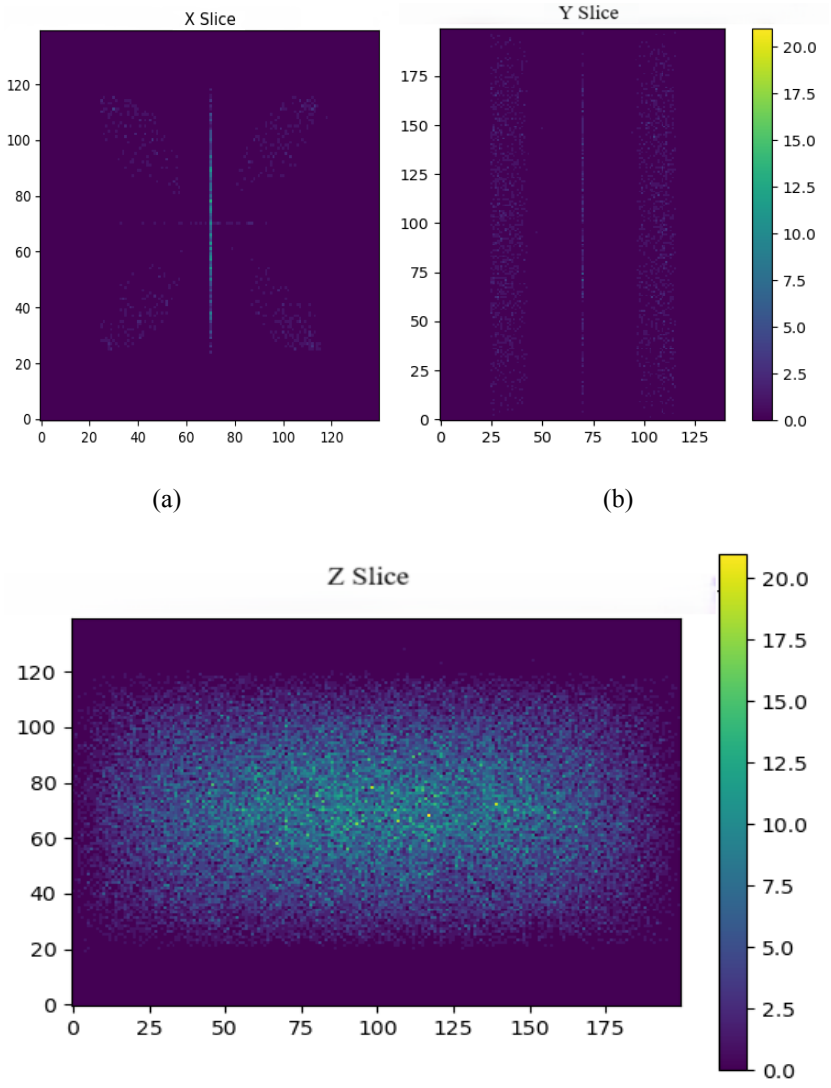

Figure 6. Density map reconstruction using the straight-line method: (a) YZ plane slice; (b) ZX plane slice; (c) XY plane slice.

The result of voxel slices in Fig.6 is completely different from what we initially expected. The initial expectation of the results was slices with a similar visual in Fig.12

4.2 POCA

Similar results are also obtained for POCA method.

4.2.1 3d ground truth simulation vs POCA simulation

While going through the phase of restriction, the ground truth points are used; they are termed as the transport points, which are physically applied while enforcing and verifying the fidelity of the reconstruction algorithms. The transport points show the actual paths of the Muons within the container, enhancing the availability of more information in reconstruction. By this, we can calculate the error rate between the paths that are made of transport points and the implemented reconstruction method point. In Fig.7, the visual comparison between the actual path (a) and the POCA path(b) of one muon is demonstrated.

[a]

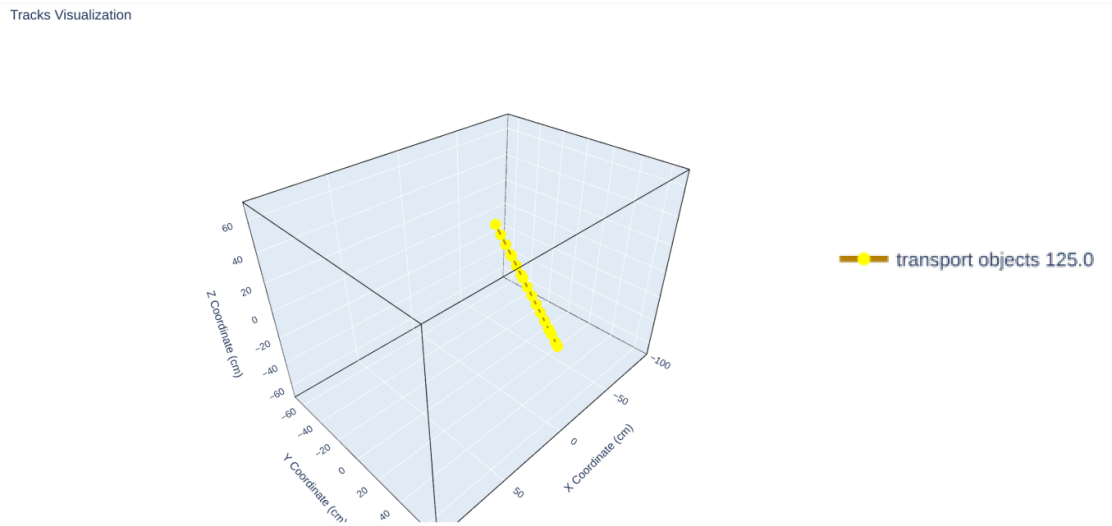

[b]

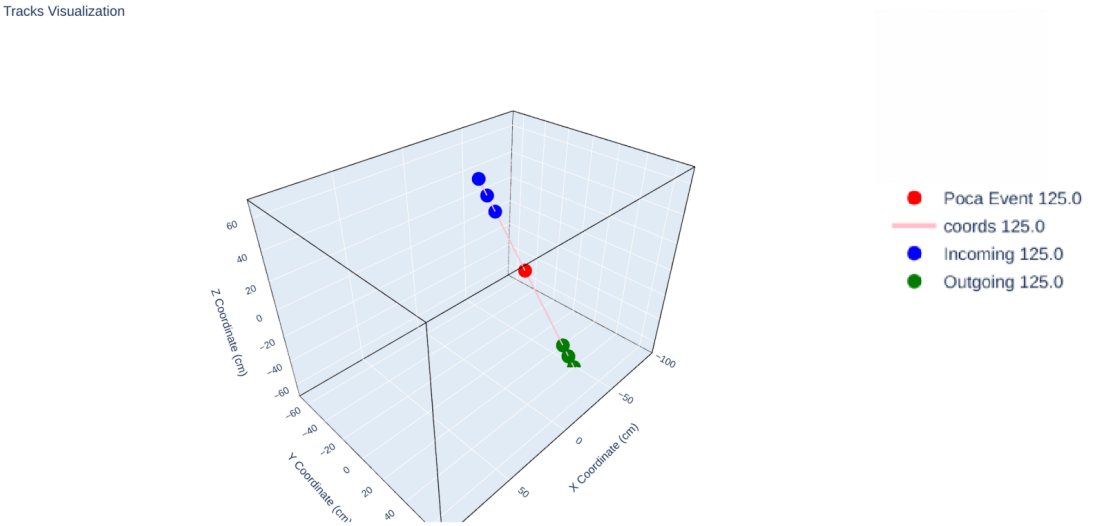

Figure 7. The visual comparison between the actual path and the POCA path. (a) the actual path; (b)the POCA path

The Actual path and POCA Path are also visually too similar in Fig.7. As well as these, the visual comparisons for other Muon examples also show similar results, which were expected after seeing the results with the straight line method.

4.2.2 The error rate between the actual path and the POCA path

The differences between the fitted lines on the POCA muon paths and the actual muon paths are also measured. In the Table.2 The average error rate in centimeters between the actual path and the POCA path is demonstrated.

Event_id	Average error
5	0.00745
9	0.46726
38	0.040083
79	0.006816
125	0.014901
741	0.029891
1148	0.05636
1943	0.428439
2208	0.131857
2484	1.37685

Table 2. The average error rate between actual and POCA paths in centimeters(cm)

The results are in the Table.2 shows how the actual and POCA paths are also similar, as the error rates are too low. This outcome also corresponds to the 3D visual comparison in Fig.7.

4.2.3 The density map with voxel slices

In Fig.8, the voxel slice examples in XY, YZ, and ZX are demonstrated for visualizing the reconstruction with the POCA Method.

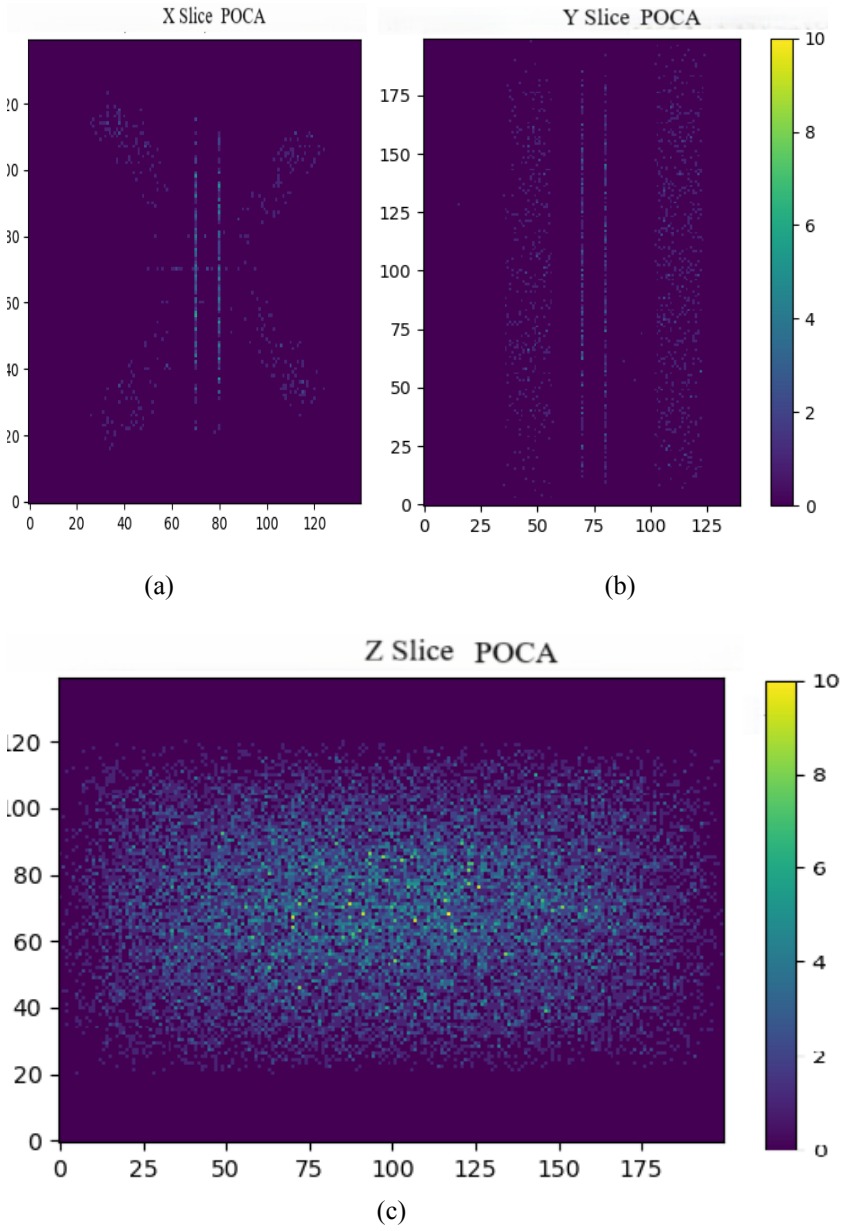

Figure 8. Density map reconstruction using the POCA method: (a) YZ plane slice; (b) ZX plane slice; (c) XY plane slice.

Just like the result of voxel slices in Fig.6, the results in Fig.8 are also completely different from what we initially expected.

4.3 MLEM

Unlike the other methods, different and better results are obtained with MLEM method

4.3.1 The density map with voxel slices

In Fig.9, the voxel slice examples in XY, YZ, and ZX are demonstrated for visualizing the reconstruction with the POCA Method.

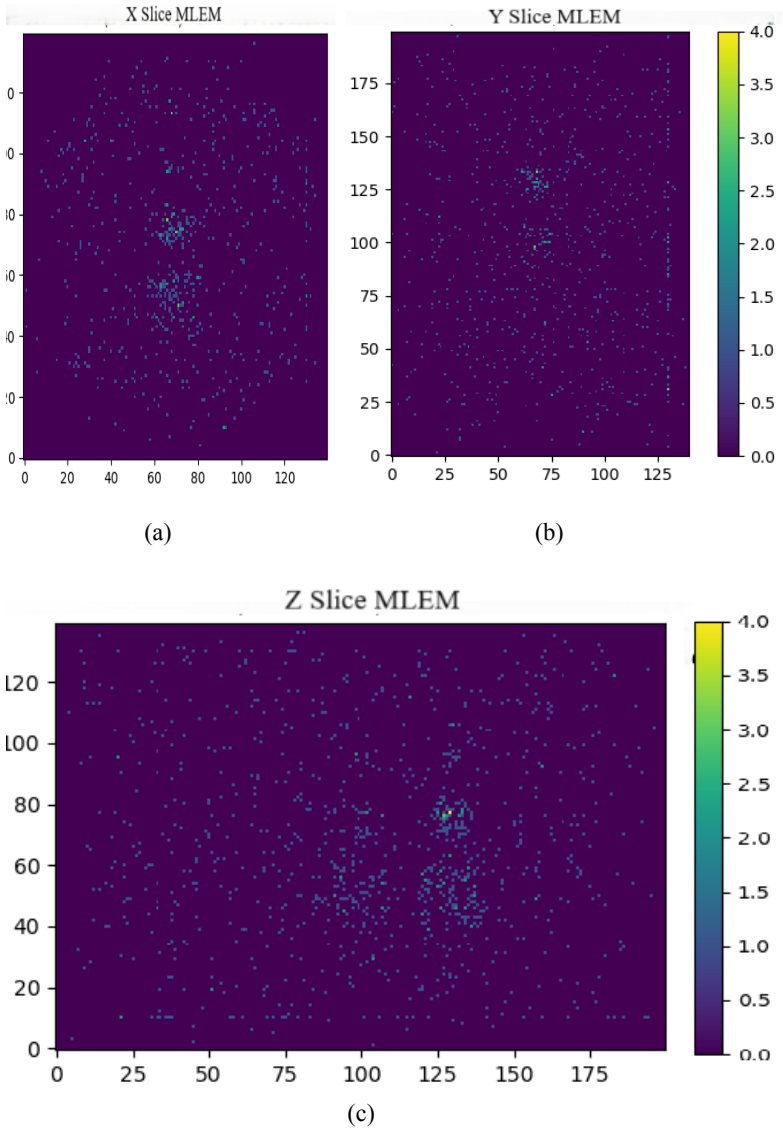

Figure 9. Density map reconstruction using the MLEM method: (a) YZ plane slice; (b) ZX plane slice; (c) XY plane slice.

The results in Fig.9 are at least able to meet our expectations. The results can mimic a similar visual of simulated objects in Fig.12

4.3.2 3D log map for MLEM grid voxel

3D Log density map is demonstrated in Fig.10 to show a better visualization of reconstruction with MLEM method.

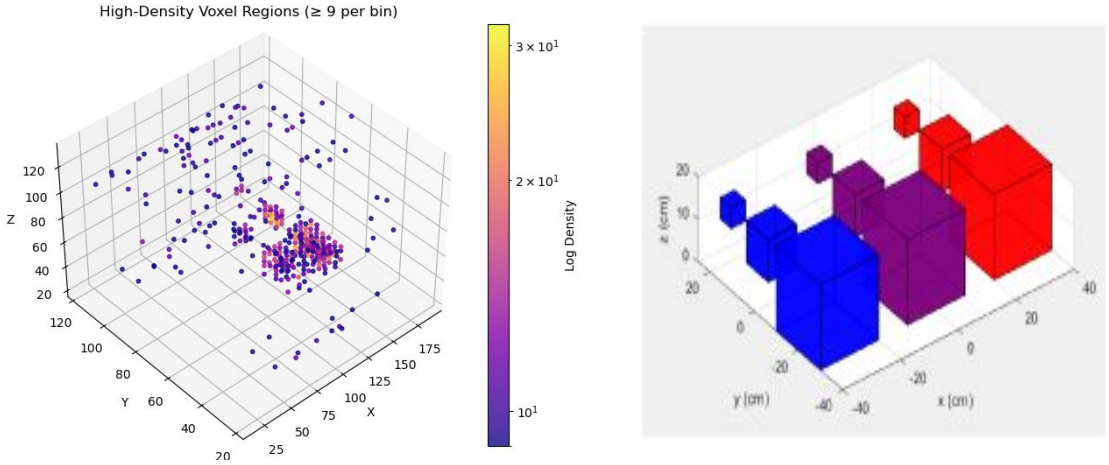

(a) (b)

Figure 10. (a) 3D Log density map for MLEM grid voxel;(b) Isometric View of the Simulated Object;

The big boxes with high Z value and middle Z value in Fig.10 (b) can be seen clearly in Fig.10 (a), which shows the isometric view of the Log density map.

4.4 Discussion

Critical inconsistencies are identified through the analysis of the results of reconstruction with POCA, Straight Line, and MLEM. The results indicate several problems in the reconstruction process of 2d voxel slices and unusual characteristics of Ground truth data.

4.4.1 Ground Truth data vs Straight line and POCA

Generally, the points of POCA and Straight line, and Incoming and Outgoing points correspond to the Ground Truth Data, which can be seen from the low average error rates in Table 1 and Table 2. As well as these, the example outputs of 3d pictures in Fig.5 and Fig.7 are helpful to support this hypothesis. But the ground truth data, which should show the actual paths of the muons in the GEANT4 simulation, mostly contains smooth and almost straight paths of the muons. This is abnormal and does not correspond to the expected path that should include some degree of scattering and curvature. This indicates that there is a possibility of errors while simulating the object in Geant4 simulation.

4.4.2 Reconstructed Voxel Slices of Straight Line and POCA Methods

The voxel slices of the Straight line and POCA methods also demonstrate unexpected results, indicating problems with the simulated data being too noisy and therefore not very useful for the Straight line and POCA Methods.

4.4.3 The analysis of the third method (MLEM)

As illustrated in Figures 9 and 10, MLEM yielded more precise and realistic reconstructions as compared to aligning with simulated objects. This implies greater sensitivity towards the limited degree of scattering data available. Nonetheless, MLEM still did not manage to capture low-Z value boxes and all small boxes due to poorly simulated scattering angles within the dataset and the need for more time to apply MLEM.

5 Methodology

5.1 Research Methods

Reenactment of Muon Tomography Information

The GEANT4 toolset is utilized to recreate the muon intuitive interior of the item of interest. GEANT4 could be a molecular transport reenactment program that gives precise modeling of muon scattering instruments. The object's shape, the materials that make up the thing, and the parameters for the approaching muon bar are all characterized as portions of the reenactment setup. The directions, energy deposition, and diffusing points of the muons, as they go through the proton, are included within the yield information obtained by GEANT4.

Application of Reconstruction methods

Python is used to execute reconstruction methods. To handle the reenacted muon tomography information and revamp the object's basic structure, three diverse methods—POCA, Straight Line and MLEM are coded. To discover scrambling centers, the POCA procedure computes the point of closest approach between entering and leaving muon directions. Straight Line Strategy assumes that muons pass through a thing in a straight line. The scrambling location is decided by taking the midpoint of the muon directions, which is the first outgoing and last incoming point. With each cycle, the MLEM approach refines the picture in an effort to maximize the chance that the observed information fits the demonstration.

5.2 Research Tools

All of the practical work has been done on a Computer with an Intel i7 10th generation, Nvidia GTX 1660 Ti 6 GB graphics card, and 16 GB DDR5 ram. Codes for all of the methods are run for the same 5 hours.
Python Programming Language: The reconstruction methods are executed

in Python. Capacities for data handling, picture making, and performance assessment are all included within the codebase. Matplotlib is utilized to visualize the results of numerical computations performed with libraries like NumPy and SciPy. Besides these, handwritten scripts are made to oversee the simulation process and handle information input, and yield.

Reading and processing data: The pandas package is used to read and process large CSV files that are filled with muon tracking data. The readcsvfileconcurrent function uses the ThreadPoolExecutor to concurrently process data and block reads using this methodology, it is possible to efficiently analyze large datasets.

Sort Data: The 'Sortdata' function is used to sort the data according to Eventid then Trackid.

Voxel grid modeling: The voxel grid of an object is simulated by the function 'Adpointstoavoxelgrid' which describes the muon-object interaction. We use simulated scattered events to determine the points of intersection between the muon's track and a voxel's boundary, and then we increment the counter for that voxel.

Difference between two points: The 'diff' function helps me to find the distances between points in the x, y, and z coordinates of a trajectory. It helps me to detect significant changes in direction. It is very helpful to make a distinction between incoming and outgoing. I also use it to calculate the distance between incoming points and outgoing points separately. The distance between incoming sensors is 10 cm^3, and similarly for outgoing.

Selecting Incoming and Outgoing Points: The function serves to find the incoming and outgoing points based on calculating the distances between points and finding the biggest distance among them, which I call the change index. The points before the change index are accepted as Incoming points. Others accepted as outgoing points.

Best line point selection: Fits a line toward the best subset of points (best line) using the RANSAC algorithm. Three incoming points and three outgoing points are chosen in cases where the data contains more than three incoming or outgoing points.

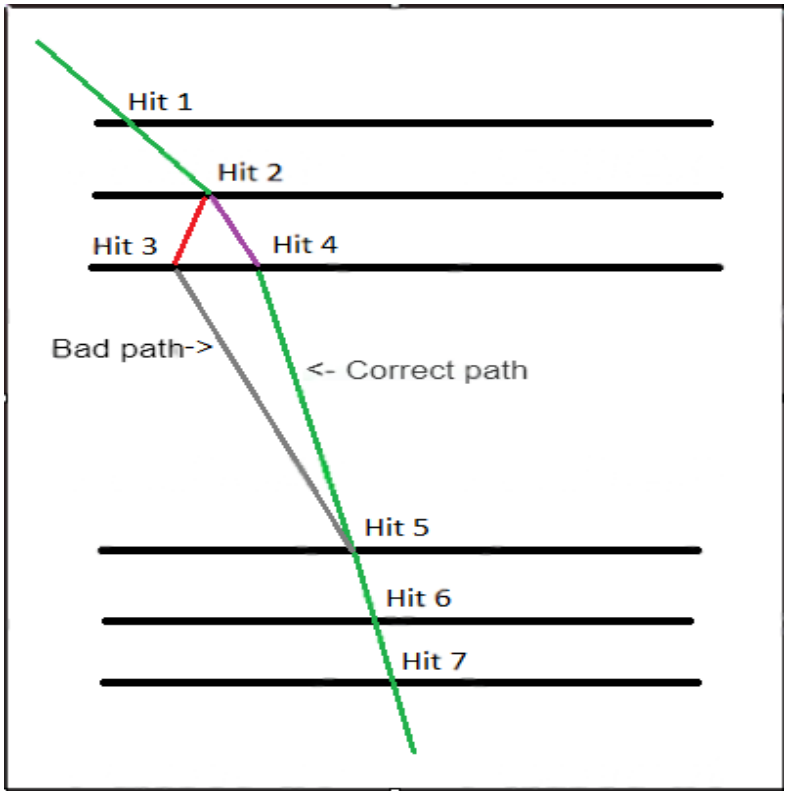

Figure 11. The Best line selection

Fig.11 shows the visualization of the purpose behind this function, as we have 4 incoming points and we want to choose the best three out of them.

Visualization and Analysis: To obtain visualization of newly created images containing slice views, the saveslices routine utilizes the Matplotlib and Plotly packages. These features allow detailed inspection of the reconstruction results by providing 2D slices of the voxel grid.

5.3 Research Object

The object of this thesis is to specifically evaluate three methods for muon tomography reconstruction and focuses on.

Simulated Object

This paper simulates muon tomography with a known internal structure through a virtual object. It aims to set an interesting degree of variability for object densities and complexities. These will work to thoroughly test both the robustness and accuracy of the reconstruction methods presented in this paper: POCA, Straight Line, and MLEM

Object Specifications

The simulations are made for three different objects of cubic shape with three different densities. Each has its center in the Volume of Interest (VOI). The specifications of the cubes are presented below:

Cubes with Sizes:

- 5x5x5 cm
- 10x10x10 cm
- 20x20x20 cm

Materials

- Very Dense (e.g., Iron - Fe): Represented in red.
- Medium Density (e.g., Flour or another substitute for cocaine): Represented in violet.
- Material Close to Air Density (e.g., Cotton): Represented in blue.
- The 10x10x10 cm cube is central in VOI, to keep the simulation conditions constant for different scenarios.

Simulation Setup

The simulated object forms part of a detailed setup of a muon tomography experiment. It was developed using the GEANT4 toolkit, which accurately models the pass-through of particles in matter. The setup consists of six sensors above and below the object, with three locations above and three below. In this way, the sensors can detect the points of intersection of the particles created. The particles simulated are muons. Of all the points involved, only the ones that determine the muon tracks are recorded. The sensors are spaced 10 cm apart for reconstruction.

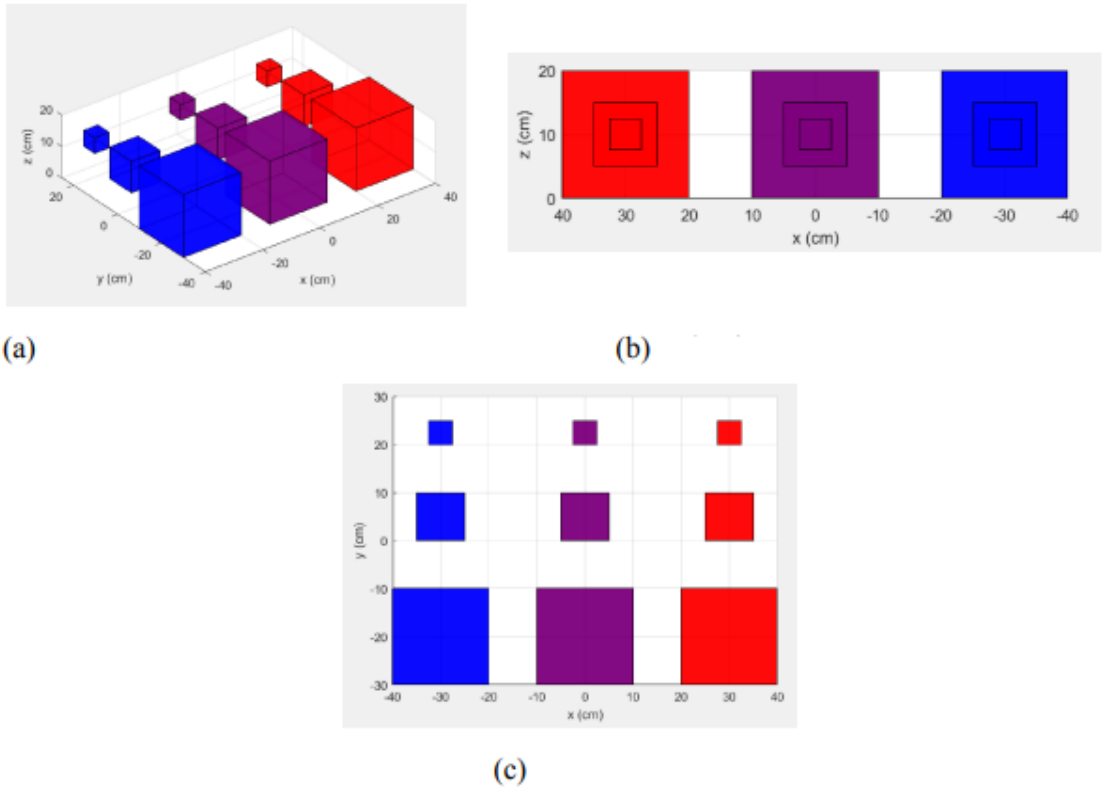

Figure 12. (a)Isometric View of the Simulated Object; (b) Side View of the Simulated Object; (c) Top View of the Simulated Object

Isometric View: An overall view in 3D space of the setup helps to confirm the correct centering of the VOI.

Side View: A view of the vertical alignment of the sensors and objects used to check the 10 cm spacing.

Top View: A view of a cross-section of the setup in the horizontal plane. This also confirms that The sensor is correctly arranged around the VOI.

Simulation Parameters: The simulation is run using parameters that guarantee at least What is collected is for a real measurement.

Exposure Time: At least 1 h for the muon interaction events collected to allow proper reconstruction.

Muon Flux: The ability to tune the flux to simulate the expected cosmic-ray muon exposure rate.

Data Recording: High-resolution tracking of muon trajectory, scattering angles, and energy deposition. Having this level of detail in the simulated object and setup, this thesis hopes to be a well-established yardstick using which the POCA, Straight Line, and MLEM reconstruction methods are compared. The structured and controlled simulation environment allows benchmarking of the performance metrics and draws meaningful conclusions on the method's applicability in practical muon tomography.

Muon Tomography Data: An output of GEANT4 simulation includes the trajectory and scattering angle of muons when passing an object's model. To create the muon paths, the above data are gathered for six virtual sensors placed on either side of an object's model through which the muons are passed. The sensors are placed at a 10 cm spacing between them and provide the points at which muons intersect and thus form the basis through which muon paths will be developed. The sensors' output is analyzed for both an incoming and an outgoing trajectory, as well as the points of scatter.

5.4 Research Materials

The muon interaction data are being produced in the GEANT4 simulation for the main data set. This includes a detailed description of muon tracks, scattering events, and energy losses. The simulation data will be organized in a structured form so that the reconstruction algorithms can access and process it easily to produce the results. The Python code repository contains the implementation for the described POCA, Straight Line, and MLEM reconstruction techniques and scripts for simulation, data processing, and evaluating the results. The given code was properly broken down into modules, and each of them consisted of a clear part of the implementation for the reconstruction process: data preprocessing, implementation of the algorithm, and postprocessing.

Computational Resources: Large-scale simulations and handling the iterative computations as required in the MLEM algorithm are realized using high-performance computing systems, which can scope the computational needs of GEANT4 simulations and MLEM processing. Computational resources also encompass multicore processors and large memory that is required for large-scale simulations, and to handle the iterative computations as required by the MLEM algorithm.

6 Conclusion

In this thesis, we investigated and compared three muon tomography reconstruction techniques: straight line, POCA (point of closest approach), and MLEM, using voxel-based density maps and simulated muon tracking data. Analysis identified a number of key findings:

Straight Line and POCA-Line Techniques

While both approaches exhibited low average error rates with respect to the ground truth muon paths, the reconstructed muon maps were not similar to the expected output in either volumetric slice outputs. As shown in Figs. 6 and 8, neither of the two methods could generate a rich or realistic rendering for the simulated object in the box. This disagreement suggests that although the track fit is precise, the density mapping is very sensitive to noise and mismatching with the simulated scattering data.

Moreover, most of the muon tracks being almost straight in the GEANT4 ground truth, having no noticeable deflection, making the general results of reconstruction too noisy.

MLEM Method

All reconstruction results were significantly improved by MLEM (in voxel slices, as well as in 3D, log-density maps) (Figs. 9 and 10). This finding was closer to the anticipated imaging of internal features and implied higher sensitivity for subtle scattering features, as well as a better ability to resolve object shapes inside the box.

However, MLEM with manual weighting still has drawbacks, such as the inability to detect low-Z and small boxes. These issues are possibly caused by the lack of sufficient scattering information and the complexity of the heuristic MLEM computation, along with the requirement for longer

processing times to accumulate enough iterations of muon paths.

Simulation Data Issues

We conclude that the GEANT4 simulation data used as the ground truth has intrinsic problems. The lack of strong bending of muon tracks and the low amount of scattering make the recoil reconstruction ineffective. This impacts both the quality of the reconstruction and the reliability of comparisons between methods.

Final Remarks

Although MLEM was the only technique among the three with the reversible potential to model internal density distributions, the overall results were highly dependent on the quality of the simulation data.

Future work should improve the simulation environment to get better muon tracks, generating less noisy synthetic data. Additionally, real-world data can be used to validate and compare the three reconstruction methods. Stricter filters could also be applied to the scattering data to discard paths with low scattering angles—potentially improving results for Straight Line and POCA methods—but this may lead to overlooking objects with low-Z value. Also data processing and reconstruction method part of the code should be accelerated as it takes too much time to run the big data.

References

[1] L. W. Alvarez, J. A. Anderson, F. E. Bedwei, J. Burkhard, A. Fakhry, A. Girgis, A. Goneid, F. Hassan, D. Iverson, G. Lynch, *et al.*, "Search for hidden chambers in the pyramids: The structure of the second pyramid of giza is determined by cosmic-ray absorption.," *Science*, vol. 167, no. 3919, pp. 832–839, 1970.

[2] G. Saracino, F. Ambrosino, L. Bonechi, L. Cimmino, R. D'Alessandro, M. D'Errico, P. Noli, L. Scognamiglio, and P. Strolin, "Applications of muon absorption radiography to the fields of archaeology and civil engineering," *Philosophical Transactions of the Royal Society A*, vol. 377, no. 2137, p. 20180057, 2019.

[3] M. Holma, P. Kuusiniemi, M. Aittola, T. Enqvist, P. Jalas, J. Joutsenvaara, K. Loo, and A. Virkajärvi, "Muon radiography and muon tomography–the two common versions of muography, and their applications in geosciences," *THE GEOLOGICAL Society OF FINLAND*, p. 26, 2019.

[4] J. Marteau, D. Gibert, N. Lesparre, F. Nicollin, P. Noli, and F. Giacoppo, "Muons tomography applied to geosciences and volcanology," *Nuclear Instruments and Methods in Physics Research Section A: Accelerators, Spectrometers, Detectors and Associated Equipment*, vol. 695, pp. 23–28, 2012.

[5] D. Carbone, D. Gibert, J. Marteau, M. Diament, L. Zuccarello, and E. Galichet, "An experiment of muon radiography at mt etna (italy)," *Geophysical Journal International*, vol. 196, no. 2, pp. 633–643, 2014.

[6] H. K. Tanaka, H. Taira, T. Uchida, M. Tanaka, M. Takeo, T. Ohminato, Y. Aoki, R. Nishitama, D. Shoji, and H. Tsuiji, "Three-dimensional computational axial tomography scan of a volcano with

cosmic ray muon radiography," *Journal of Geophysical Research: Solid Earth*, vol. 115, no. B12, 2010.

[7] R. T. Kouzes, A. Bonneville, A. Lintereur, I. Mostafanezhad, R. Pang, B. Rotter, F. Snigdha, M. Tytgat, S. Aly, B. ElMahdy, *et al.*, "Novel muon tomography detector for the pyramids," *arXiv preprint arXiv:2202.08166*, 2022.

[8] L. Thompson, J. Stowell, S. Fargher, C. Steer, K. Loughney, E. O'Sullivan, J. Gluyas, S. Blaney, and R. Pidcock, "Muon tomography for railway tunnel imaging," *Physical Review Research*, vol. 2, no. 2, p. 023017, 2020.

[9] A. Erlandson, K. Boniface, V. N. Anghel, G. Jonkmans, M. Thompson, and S. Livingstone, "One-sided muon tomography—a portable method for imaging critical infrastructure with a single muon detector," *CNL Nuclear Review*, vol. 7, no. 1, pp. 1–9, 2016.

[10] S. Riggi, V. Antonuccio-Delogu, M. Bandieramonte, U. Becciani, A. Costa, P. La Rocca, P. Massimino, C. Petta, C. Pistagna, F. Riggi, *et al.*, "Muon tomography imaging algorithms for nuclear threat detection inside large volume containers with the muon portal detector," *Nuclear Instruments and Methods in Physics Research Section A: Accelerators, Spectrometers, Detectors and Associated Equipment*, vol. 728, pp. 59–68, 2013.

[11] L. J. Schultz, K. N. Borozdin, J. J. Gomez, G. E. Hogan, J. McGill, C. Morris, W. Priedhorsky, A. Saunders, and M. Teasdale, "Image reconstruction and material z discrimination via cosmic ray muon radiography," *Nuclear Instruments and Methods in Physics Research Section A: Accelerators, Spectrometers, Detectors and Associated Equipment*, vol. 519, no. 3, pp. 687–694, 2004.

[12] G. Jonkmans, V. Anghel, C. Jewett, and M. Thompson, "Nuclear waste imaging and spent fuel verification by muon tomography," *Annals of Nuclear Energy*, vol. 53, pp. 267–273, 2013.

[13] D. Poulson, J. Bacon, M. Durham, E. Guardincerri, C. Morris, and H. R. Trellue, "Application of muon tomography to fuel cask monitoring," *Philosophical Transactions of the Royal Society A*, vol. 377, no. 2137, p. 20180052, 2019.

[14] B. Lefevre, J. Vogel, H. Gomez, D. Attié, L. Gallego, P. Gonzales, B. Lesage, P. Mas, and D. Pomarède, "3d reconstruction of a nuclear reactor by muon tomography: Structure validation and anomaly detection," *PRX Energy*, vol. 4, no. 1, p. 013002, 2025.

[15] P. Checchia, "Review of possible applications of cosmic muon tomography," *Journal of Instrumentation*, vol. 11, no. 12, p. C12072, 2016.

[16] C. J. Rhodes, "Muon tomography: looking inside dangerous places," *Science progress*, vol. 98, no. 3, pp. 291–299, 2015.

[17] L. J. Schultz, G. S. Blanpied, K. N. Borozdin, A. M. Fraser, N. W. Hengartner, A. V. Klimenko, C. L. Morris, C. Orum, and M. J. Sossong, "Statistical reconstruction for cosmic ray muon tomography," *IEEE transactions on Image Processing*, vol. 16, no. 8, pp. 1985–1993, 2007.

[18] S. N. Axani, "The physics behind the cosmicwatch desktop muon detectors," *arXiv preprint arXiv:1908.00146*, 2019.

[19] A. S. Georgadze and V. A. Kudryavtsev, "Geant4 simulation study of low-z material detection using muon tomography," *Journal of Instrumentation*, vol. 18, no. 12, p. C12014, 2023.

[20] W. Zeng, M. Zeng, X. Pan, Z. Zeng, H. Ma, and J. Cheng, "Principle study of image reconstruction algorithms in muon tomography," *Journal of Instrumentation*, vol. 15, no. 02, p. T02005, 2020.

[21] M. Stapleton, J. Burns, S. Quillin, and C. Steer, "Angle statistics reconstruction: a robust reconstruction algorithm for muon scattering

tomography," *Journal of instrumentation*, vol. 9, no. 11, p. P11019, 2014.

[22] G. Yang, T. Clarkson, S. Gardner, D. Ireland, R. Kaiser, D. Mahon, R. A. Jebali, C. Shearer, and M. Ryan, "Novel muon imaging techniques," *Philosophical Transactions of the Royal Society A*, vol. 377, no. 2137, p. 20180062, 2019.

Appendix

A GitHub Repository

The full source code used in this thesis, including simulation scripts, reconstruction methods (POCA, Straight Line, MLEM), and data processing tools, is available at the following GitHub repository:
https://github.com/rufetabdullayev/Thesis

I. Licence

Non-exclusive licence to reproduce thesis and make thesis public

I, **Rufat Abdullayev**,
*(*author's name)

1. herewith grant the University of Tartu a free permit (non-exclusive licence) to

   reproduce, for the purpose of preservation, including for adding to the DSpace digital archives until the expiry of the term of copyright,

   The Comparison of three Reconstruction methods (Straight line, Point of the closest approach (POCA), Maximum likelihood expectation maximization (MLEM)),
   *(*title of thesis)

   Supervised by Leonid Zinatullin.
   *(*supervisor's name)

2. I grant the University of Tartu a permit to make the work specified in p. 1 available to the public via the web environment of the University of Tartu, including via the DSpace digital archives, under the Creative Commons licence CC BY NC ND 3.0, which allows, by giving appropriate credit to the author, to reproduce, distribute the work and communicate it to the public, and prohibits the creation of derivative works and any commercial use of the work until the expiry of the term of copyright.

3. I am aware of the fact that the author retains the rights specified in p. 1 and 2.

4. I certify that granting the non-exclusive licence does not infringe other persons' intellectual property rights or rights arising from the personal data protection legislation.

Rufat Abdullayev
20/05/2025